

Simultaneous phosphate and ammonium removal from aqueous solution by a hydrated aluminum oxide modified natural zeolite

Diana Guaya ^{a, b*}, Cesar Valderrama ^a, Adriana Farran ^a, Chabaco Armijos ^b, José Luis Cortina ^{a, c}

^a Department of Chemical Engineering, Universitat Politècnica de Catalunya-Barcelona Tech (UPC), Barcelona, Spain

^b Departament of Chemistry, Universidad Técnica Particular de Loja, Loja, Ecuador

^c Water Technology Center CETaqua, Barcelona, Spain

*Correspondence should be addressed to: Diana Guaya

Email: deguaya@utpl.edu.ec

Abstract

A natural zeolite (Z-N), rich in clinoptilolite, was modified (Z-AI) by incorporation of hydrated aluminum oxide (HAIO) for the simultaneous phosphate and ammonium removal. The incorporation of surface hydroxyl groups ($\cong\text{Al-OH}$) into the zeolite structure, as active groups for phosphate removal, was characterized by acid-base titrations ($\text{pH}_{\text{PZC}}=4.5\pm 0.2$). The phosphate sorption increases from 0.6 mg-P/g for Z-N up to 7.0 mg-P/g while only a slight decrease on the ammonium sorption capacity from 33 mg-N/g of Z-N to 30 mg-N/g for Z-AI was observed. The HAIO modified zeolite sorption capacity for both phosphate and ammonium was slightly reduced by common ions typically present in secondary waste water effluents. Column experiments revealed higher enrichment factor for ammonium (120) than for phosphate (50) using 1 M NaOH as elution solution. A reduction of zeolite phosphate capacity with regeneration cycles was observed.

Keywords: clinoptilolite; natural zeolite; modification; hydrated aluminum oxide; adsorption; kinetic

1. Introduction

Nitrogen and phosphorus are essential nutrients for all living forms. However, an excessive growth of algae and the consequently depletion of the dissolved oxygen is an effect of the nutrient overloading (phosphate and ammonium) in natural water bodies [1, 2]. Therefore, it has become a great challenge addressed to the simultaneous removal of both species (phosphate and ammonium) to avoid the consequences of eutrophication processes. Natural and synthetic zeolites have been widely studied for ammonium removal due to its high cationic exchange property [1, 3, 4] and they have been postulated as promissory materials for its removal from waste waters [5-8]. Zeolites and their modified forms have been widely used as effective adsorbents for waste water treatment according to their mechanical and thermal properties, capability of cation-exchange and significant worldwide occurrence. Additionally, the safety, easy operation and maintenance, low treatment costs, high selectivity and the release of non-toxic exchangeable cations (K^+ , Na^+ , Ca^{2+} and Mg^{2+}) make zeolites an attractive alternative [3, 9, 10]. Zeolite are hydrated crystalline aluminum-silicate materials with a framework structure where micro- and mesopores located by water and typically alkaline cations [11]. However, they have been rarely used for phosphate sorption due to the constant negative charge on their surface [12]. In order to improve the ion exchange capacity of natural zeolites for anionic species the incorporation or impregnation of iron and aluminum oxides, are the most widespread and excellent candidates for phosphate removal [13-18]. Zeolites exhibit different properties which depend on the geological location and they deserve a detailed characterization [19, 20]. This study describes the modification of a Slovakian natural zeolite (clinoptilolite) with Al (III) to enhance the formation of hydrated aluminum oxide (HAIO) onto the zeolite structure. Utilization of hydrated aluminum oxide in treatment processes cause difficulties in separation due to their small sizes that could be overcome by its impregnation into zeolite porous particles. No previous studies have been found about the hydrated aluminum oxide modification of a natural clinoptilolite for the

simultaneous removal of both nutrients. Therefore, the findings of the present work provide insight into the simultaneous phosphate and ammonium sorption potential of hydrated aluminium oxide supported on a clinoptilolite and its regeneration for re-use in sorption and desorption cycles as low cost materials for industrial and domestic waste water treatment applications. The objectives of this study are: (i) synthesize supported hydrated aluminum hydroxide zeolites, (ii) characterize the modified zeolite, (iii) study the influence of pH and ions concentration on zeolites removal capacity, (iv) determine the equilibrium and kinetic sorption parameters, (v) determine the sorption selectivity in front of common ions in waste waters effluents and, (vi) evaluate their performance (sorption and desorption) on column experiments.

2. Materials and methods

2.1. Impregnation of hydrated aluminum oxide onto a natural zeolite

A natural zeolite (Z-N) obtained from Zeocem Company, Slovakian Republic was used. Samples were washed with deionized water and dried in an oven at 80 °C for 24 hours. Particles below 200 µm mesh were used for batch experiments and particles between 800 – 1200 µm mesh were used for column experiments. Z-N was modified to the aluminum form by using an adaptation of the method reported by Jiménez-Cedillo [14]. Thirty grams of natural zeolite were treated with 250 mL of NaCl (0.1 M) two consecutive times under reflux conditions for 4 hours. Then, the zeolite in the sodium form (Z-Na) was washed with ~1500 mL of deionized water until no chloride was detected by the AgNO₃ test. Thirty grams of sodium zeolite (Z-Na) were treated two consecutive times with 250 mL of AlCl₃ (0.1 M) under reflux for 4 hours. The aluminum zeolite (Z-Al) was washed using ~1500 mL of deionized water until no chloride was detected by the AgNO₃ test. Finally, it was dried in an oven at 80 °C for 24 hours.

2.2. Physicochemical characterization of the zeolites

Z-N, Z-Na and Z-Al were characterized by X-ray diffraction (XRD) using a powder X-ray Diffractometer (D8 Advance A25 Bruker). Samples morphology and chemical composition were analyzed by a Field Emission Scanning Electron Microscope (FSEM) (JEOL JSM-7001F) coupled to an Energy Dispersive Spectroscopy system (Oxford Instruments X-Max). Samples composition reported are the average of at least four analyses for each sample. Infrared absorption spectra were recorded with a Fourier Transform FTIR 4100 Jasco spectrometer in the range of 4000 – 550 cm⁻¹ range. The specific surface area of Z-N and Z-Al was determined by the nitrogen gas sorption method on an automatic sorption analyzer (Micrometrics). The essays were replicated four times for each sample and the average data are reported. The point of zero charge (PZC) of Z-N and Z-Al was determined by the pH drift method [21, 22]. An amount 0.1 g of zeolite was equilibrated in 25 mL of deionized water and 0.01 and 0.05 M NaCl solutions (pH from 2 to 11) for 24 hours at 200 rpm and 21±1 °C. The final pH was measured in a Crison GLP21 potentiometer, and the PZC was determined as the pH at which the addition of the sample did not induce a shift in the pH ($\Delta\text{pH}=\text{pH}_f-\text{pH}_i=0$). The CIP method, common intersection point of potentiometric titration curves obtained at three ionic strengths was also used [23-25]. An amount of 0.1 g of zeolite was equilibrated with 25 mL of solution at three different ionic strengths (0.01, 0.05 and 0.1 M NaCl) during 24 h at 200 rpm and 21±1°C. After the equilibration the suspension was basified to pH 11 using 0.1 M NaOH. The suspension was titrated until pH ≈ 3, with 0.01 M HCl using an automatic titrator (Mettler Toledo). The net surface charge is correlated with PZC from the titration data for the adsorbed amounts of [H⁺] and [OH⁻] ions. Therefore, titration curves of different ionic strength would intersect at pH = pH_{PZC}. The surface charge was calculated from the Eq. 1 [26].

$$b = C_b - C_a + [H^+] - [OH^-] \quad (1)$$

where: *b* (mol/g) is the net hydroxide ions consumed, *C_b* and *C_a* (mol/L) are the base and acid concentrations, respectively and [H⁺] and [OH⁻] denote the protons and hydroxide concentration

calculated from the measured solution pH for a given mass of zeolite (g) and a given volume of volume of solution (L). All measurements were performed in triplicate and the average value was reported.

2.3. Equilibrium and kinetic batch sorption studies

Batch equilibrium sorption experiments were carried out using standard batch methodology described elsewhere [8]. Given volumes (25 mL) of phosphate (P) and ammonium (N) aqueous solutions were shaken overnight with weighed amounts of dry samples (particle size < 200 μm) in polyethylene tubes using a continuous rotary mixer. Three different types of experiments were conducted:

i) Sorption capacity as function of phosphate and ammonium concentration: 0.25 g of Z-N and Z-Al samples were added to solutions in the concentration range: 1 - 2000 mg-P/L and 10 – 5000 mg-N/L, without pH adjustment.

ii) Sorption capacity as function of equilibrium pH: 0.1 g of Z-Al sample was equilibrated in solutions containing 25 mg-P/L and 25 mg-N/L. The pH was adjusted from 2 to 11 (using 0.1 M HCl/NaOH).

iii) Sorption capacity as function of phosphate and ammonium concentration in the presence of individual and mixtures of common competing ions present on waste water effluents: 0.1 g of Z-Al sample is added to 25 mg-P/L, 25 mg-N/L and individual competing ion (25 mg/L) solutions without pH adjustment. Also, the interference ions concentrations were fixed taking as reference the average annual composition of the stream from a tertiary treatment including a reverse osmosis step at the El Prat waste water treatment plant (Barcelona – Spain). The anions solution composition was: chloride (625 mg/L), bicarbonate (325 mg/L), sulfate (200 mg/L) and nitrate (30 mg/L) (prepared from the corresponding sodium salts). The cations solution composition was: sodium (260 mg/L), calcium (160 mg/L), magnesium (50 mg/L) and potassium (40 mg/L) (prepared from corresponding chloride salts). Then, 0.25 g of Z-Al sample was equilibrated in solutions ranging 1 - 2000 mg-P/L and 10 – 5000 mg-N/L and the mixture of competing ions.

iv) Batch kinetic sorption experiments were performed by addition of 0.1 g of Z-Al in solution containing 20 mg-N/L and 10 mg-P/L. Tubes were withdrawn sequentially at given times. All tests were performed by triplicate at 200 rpm and room temperature (21 ± 1 °C) and the average data are reported. Before to be analyzed samples were centrifuged for 10 min and filtered using cellulose nitrate membrane filters (45 μ m). The total concentrations of phosphate and ammonium ions in the initial and remaining aqueous solution were determined.

2.4. Phosphate speciation in loaded Z-Al samples by fractionation assays.

The phosphorus speciation was performed based on an adaptation of the sequential extraction protocol [27] with three extraction steps. Z-Al samples (0.25 g) were equilibrated in 25 mL of solution containing 25 mg-P/L at 200 rpm for 24 h. Loaded samples were filtered, washed with deionized water and dried. The fraction of loosely bound phosphorus was extracted in two consecutive extractions by 0.25 g of loaded Z-Al sample in 20 mL of 1 M NH_4Cl at pH 7. Then, the phosphorous bound to iron and aluminum components was determined by means of two consecutive extractions in 20 mL of 0.1 M NaOH followed by extraction in 1 M NaCl. In the third step, the potential content of phosphorus immobilized in the form of calcium and magnesium was extracted in two consecutive times in 20 mL of 0.5 M HCl. Finally, residual content is determined by the mass balance between the phosphorus adsorbed and the extracted fractions. Tests were performed in triplicate at 21 ± 1 °C and the average values are reported.

2.5. Phosphate and ammonium batch desorption studies

Samples of Z-Al (0.5 g < 200 μ m) were saturated in 25 mL of solution containing 25 mg-P /L and 25 mg-N/L at 200 rpm for 24 h. Z-Al samples were separated by filtration and rinsed several times with deionized water for the desorption trials. The desorption studies were performed by adding 0.5 g of the saturated zeolite into 25 mL of elution solution at 200 rpm for 24 h. Solutions of NaOH (1 M), NaHCO_3 (0.1 M), Na_2CO_3 (0.1 M) and $\text{NaHCO}_3/\text{Na}_2\text{CO}_3$ (0.1 M) were evaluated. Tests were

performed in two sorption – desorption cycles by triplicate at 21 ± 1 °C and average values are reported.

2.6. Phosphate and ammonium sorption and desorption column studies

Samples of Z-Al (<800 μm particles) were packed in a glass column (15mm inner diameter and 100mm length). Initially, the column was equilibrated with ~20 BV of deionized water. The feed composition was established taking as reference the expected values of effluents streams after secondary treatment from the El Prat waste water treatment plant (Barcelona – Spain). The feed solution composition was: phosphate (12.5 mg/L), ammonium (25 mg/L), chloride (312.5 mg/L), bicarbonate (162.5 mg/L), sulfate (10 mg/L), nitrate (15 mg/L), sodium (130 mg/L), calcium (80 mg/L), magnesium (25 mg/L) and potassium (20 mg/L). The solution with and without competing ions was supplied in countercurrent through the column at EBHRT of 4 minutes. After saturation the Z-Al was regenerated with 1 M NaOH solution at EBHRT of 13 minutes.

2.7. Analytical methods

Phosphate (P) and ammonium (N) concentration were determined based on the Standard Methods [28]. P-PO_4^{3-} was determined by the vanadomolybdophosphoric acid colorimetric method (4500-P C) in a Shimadzu UVmini-1240 UVvis spectrophotometer. N-NH_4^+ was determined by the ammonia-selective electrode method (4500-NH3 D). A Hach 51927-00 ammonia gas sensing gas combination electrode was used for this purpose. Ions were determined using a Thermo Scientific Ionic Chromatograph (Dionex ICS-1100 and ICS-1000). On the completion of the batch experiments, samples of the loaded zeolites were examined by field scanning electron microscope (FSEM-EDX) and mineral phases were identified by X-Ray Diffractometry (XRD).

3. Results and discussion

3.1. Materials characterization of hydrated aluminum oxide zeolites

XRD patterns of Z-N, Z-Na and the modified hydrated aluminum oxide zeolite (Z-Al) are shown in supporting information Figure S1. Clinoptilolite was found to be the major component of Z-N, but also small amounts of other crystalline phases as quartz and albite were detected. In this study Z-Na is considered as an intermediary step of the zeolite modification process, due to the easily sodium removal in ion exchange applications [29]. The presence of crystalline aluminum phases (e.g. hydrated aluminum oxide) was not identified in Z-Al samples as it was described by Jimenez-Cedillo about the formation of amorphous oxide species on a modified zeolite surface [14, 15, 30]. For Z-Al only differences on the reflexions intensity but not on their positions were observed. This fact is attributed to the occupation of aluminum ions in the cation exchange sites of the zeolitic structure after the AlCl_3 treatment. However, some characteristic reflexions (2θ at 9.9° , 11.2° , 17.3° , 22.5° and 32.0°) for clinoptilolite were not affected through modification of Z-Na and Z-Al. The specific surface area of Z-N is slightly reduced from $19.8 \pm 0.3 \text{ m}^2/\text{g}$ to $17.8 \pm 0.1 \text{ m}^2/\text{g}$ of Z-Al as consequence of the impregnation of hydrated aluminum oxide and the interaction between compensating cations (e.g. Al(III)) and water molecules which are coordinated in the zeolite framework [31].

The FSEM – EDX analyses revealed the presence of O, Na, Mg, Al, Si, K, Ca and Fe as the main elements on the zeolites composition (Table 1). In Z-Na, the sodium content increase from 0.4 % to 1.5 % and a decrease of potassium and calcium content was observed due to the exchange with sodium ions. As well as, in Z-Al the aluminum content increased from 5.3 % to 6.3 % with a reduction of sodium and magnesium content was observed from 1.5 % to 0.9 % and 0.4 % to 0.2 % as consequence of the ion exchange occur between these cationic species and aluminum.

Element	Z-N	Z-Na	Z-Al
O	57.8 ± 2.6	60.3 ± 1.4	58.1 ± 1.5
Na	0.3 ± 0.0	1.5 ± 0.1	0.9 ± 0.3
Mg	0.4 ± 0.1	0.4 ± 0.0	0.2 ± 0.2

Al	5.3 ± 0.2	5.3 ± 0.0	6.3 ± 0.4
Si	29.7 ± 1.7	29.1 ± 1.5	30.3 ± 0.5
K	2.9 ± 0.5	1.8 ± 0.2	2.2 ± 0.3
Ca	1.9 ± 0.3	1.1 ± 0.1	1.3 ± 0.5
Ti	0.2 ± 0.2	< loq*	< loq*
Fe	1.6 ± 0.4	0.5 ± 0.0	1.1 ± 0.3

*loq: limit of quantification

Table 1. Chemical composition (wt. %) of the zeolitic materials: Natural zeolite (Z-N), sodium zeolite form (Z-Na) and hybrid hydrated aluminum oxide zeolite (Z-Al).

FSEM images showed the networks of crystal clusters for the Z-N (supporting information Figure S2a) with homogeneous crystal size distribution. It is observed for clinoptilolite the characteristically plate-like morphology crystals and large cavities and entries to the channels inside the zeolite framework in accordance to previous reports [32]. The existence of lamellar crystals and small particles covering the surface is observed in Z-Na and Z-Al (supporting information Figure S2b,c) confirms the surface modification achieved in the clinoptilolite after the sodium and aluminum treatments.

The acid - base characterization provides a pH_{PZC} of 4.5 ± 0.2 for Z-Al (Figure 1) by both methods employed in comparison with Z-N with a value of 5.2 ± 0.2 . The decrease of the pH_{PZC} suggests that Z-Al become more acid as an effect of formation of hydrated aluminum oxide onto the zeolite after the modification with Al (III) salt. The determined pH_{PZC} is in agreement with reported values for natural zeolite (clinoptilolite) supporting mono Fe(II) (Z-Fe(II)), Al (Z-Al) and bimetallic Fe-Al (Z-Fe/Al) with pH_{PZC} values of 4.2, 4.6 and 5.2, respectively [13]. It is also in agreement with pH_{PZC} for α -Al(OH)₃(s) (pH_{PZC} 5.0) but far from the values reported for α -Al₂O₃(s) (pH_{PZC} =9.1) and for γ -AlOOH(s) (pH_{PZC} =8.2) [33].

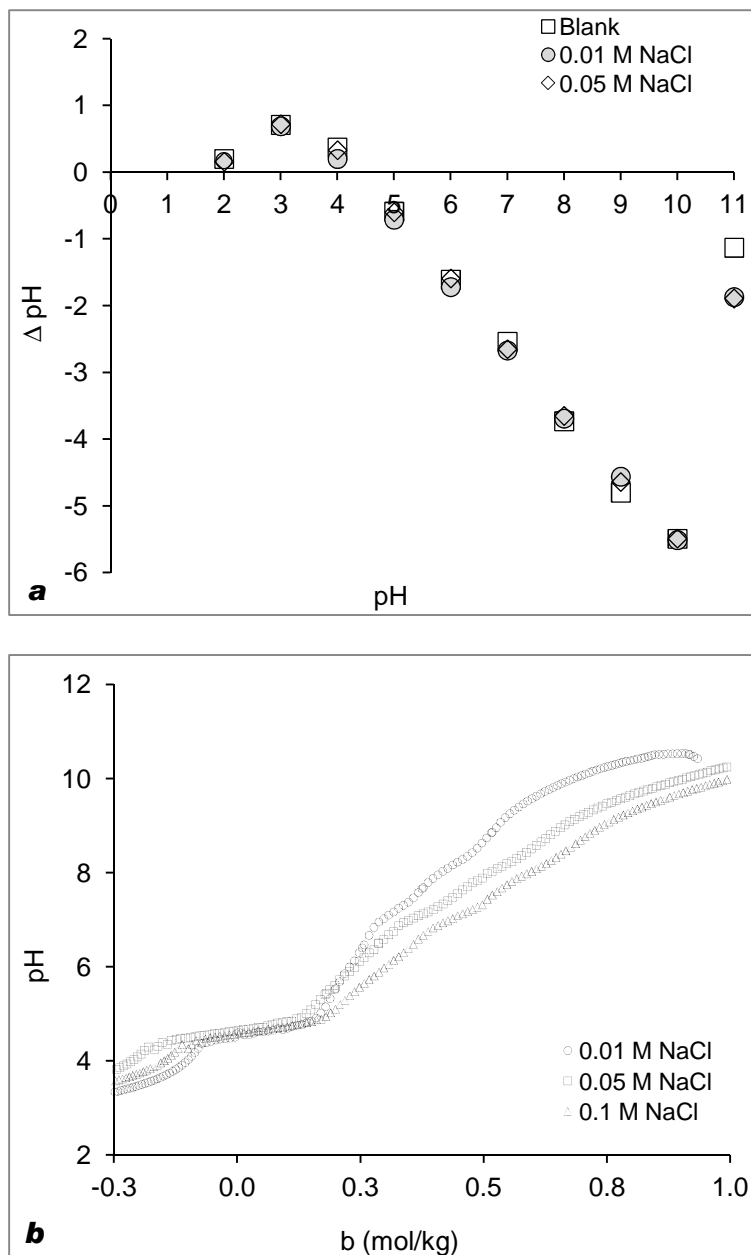


Figure 1. a) Plot of $\text{pH}_{\text{final}} - \text{pH}_{\text{initial}}$ vs initial pH of Z-Al with and without electrolyte NaCl and b) Potentiometric titration curve for Z – Al, at 0.01, 0.05 and 0.1 M NaCl.

The FTIR spectra for Z-N, Z-Na and Z-Al are shown in supporting information (Figure S3). Peaks between 798 cm^{-1} and 547 cm^{-1} are assigned to deformation vibration of OH, Al-O-Si and Si-O-Si groups. The band at $\sim 1100 \text{ cm}^{-1}$ is attributed to the stretching vibration of Si-O groups and the one at $\sim 1630 \text{ cm}^{-1}$ represents the deformation vibration of water. The peaks in the range from 3700 cm^{-1} to

3100 cm⁻¹ have been associated to the hydroxyl groups of the zeolitic structure [11, 34]. The small differences in the spectra for Z-N (Figure S3a) and Z-Na (Figure S3b) are consistent with the ion exchange reactions between cations of the same valence [35]. Contrary, after the modification with a trivalent cation (Al (III)) important changes in the zeolite structure are observed on the Z-Al spectra (Figure S3c), with new peaks at 1396 cm⁻¹, 1455 cm⁻¹ and 1541 cm⁻¹ associated with the presence of the surface hydroxide groups ($\equiv\text{AlOH}$) [36-38]. The shift of the band at ~3396 cm⁻¹ in the Z-N spectra and the new band at 3616 cm⁻¹ on Z-Al spectra are attributed to hydroxyl groups associated with tetrahedral framework aluminum and octahedral non-framework aluminum oxide species [39, 40]. It results in the formation of cationic OH groups and bridging OH groups which are situated in the channels of zeolite as well as at the outer surface of particles [41]. All these changes confirm the formation of aluminum hydroxyl groups which promote the acidity increase of natural clinoptilolite as it was identified on surface layers of Z-Al in SEM analysis.

3.2. Phosphate and ammonium isotherms

The equilibrium uptake for phosphate and ammonium (q_e) was calculated by Eq. 2.

$$q_e = (C_o - C_e) \times \frac{v}{w} \quad (2)$$

where C_o (mg/L) and C_e (mg/L) represents the initial and equilibrium concentration, respectively; v (L) is the aqueous solution volume and w (g) is the mass of zeolite. The phosphate and ammonium equilibrium sorption was evaluated according to Langmuir and Freundlich isotherms by Eq. 3 and Eq. 4, respectively.

$$\frac{C_e}{q_e} = \frac{1}{K_L \cdot q_m} + \frac{C_e}{q_m} \quad (3)$$

$$\log q_e = \log K_F + \frac{1}{n} \log C_e \quad (4)$$

where q_m (mg/g) is the maximum sorption capacity and K_L (L/mg) is the Langmuir sorption equilibrium constant. K_F ((mg/g)/(mg/L)^{1/n}) is the Freundlich equilibrium sorption constant.

The phosphate and ammonium sorption data are well described by the Langmuir isotherm ($R^2 \geq 0.99$) while Freundlich isotherm ($R^2 \leq 0.97$) (Table 2 and Figure 2) provides a good description only at the lower concentration ranges. Therefore, monolayer and homogenous sorption or/and ion exchange at specific and equal affinity sites available on the zeolites surface is supposed to occur. A favorable sorption is revealed by the values of K_L (0.02 and 0.011 for phosphate and ammonium, respectively) [42]. For Z-N the maximum sorption capacities for ammonium and phosphate were found to be 33 mg-N/g and 0.6 mg-P/g, respectively; while Z-Al phosphate capacity was enhanced tenfold 7.0 mg-P/g. A small decrease of sorption capacity for ammonium (30 mg-N/g) was reported in Z-Al and consequently the increase of bonding sites for phosphate ions represents a slightly reduction for ammonium ones.

		Langmuir			Freundlich		
		q_m (mg/g)	K_L (L/mg)	R^2	K_F ((mg/g)/(mg/L) ^{1/n})	1/n	R^2
Z-N	Phosphate	0.6	0.01	0.99	0.02	0.47	0.97
	Ammonium	33	0.006	0.99	1.84	0.36	0.94
Z-Al	Phosphate	7.0	0.02	0.99	0.85	0.32	0.85
	Ammonium	30	0.011	0.99	2.64	0.32	0.92

Table 2. Isotherm parameters for phosphate and ammonium sorption on natural zeolite (Z-N) and hybrid hydrated aluminum oxide zeolite (Z-Al).

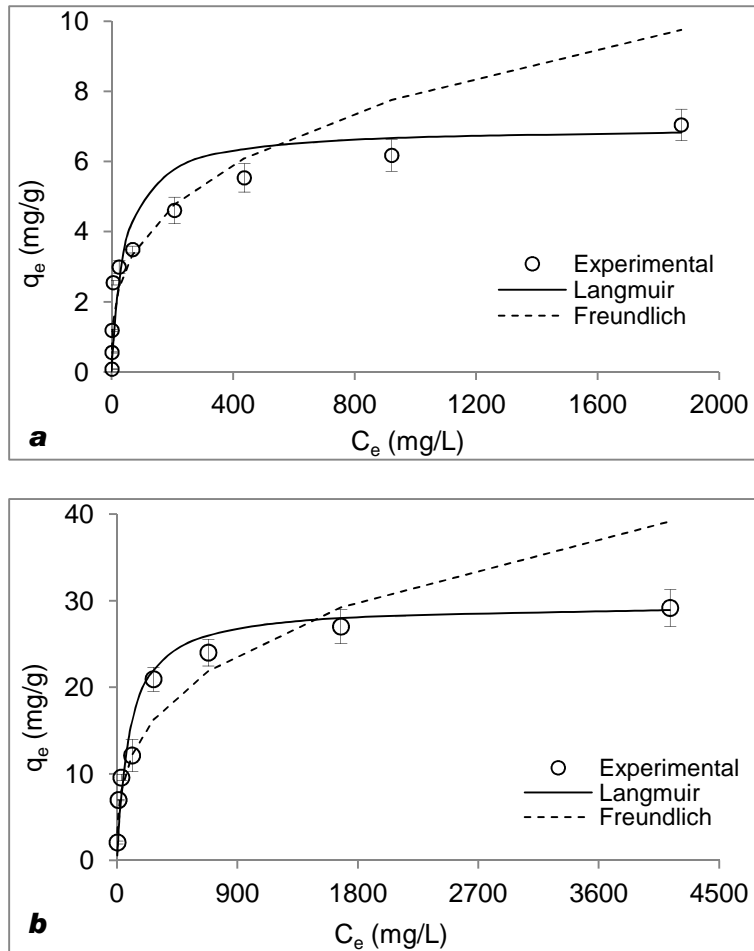


Figure 2. Experimental and theoretical equilibrium isotherms for a) phosphate and b) ammonium removal by hybrid hydrated aluminum oxide zeolite (Z-Al) at $21 \pm 1^\circ\text{C}$. Sorption experiments were carried at constant equilibrium pH 4.2 ± 0.2

Sorption of ions with acid base properties (e.g. phosphate and ammonium) on adsorbent surface sites occurs by specific and/or nonspecific interactions. The specific type of sorption takes place by ligand exchange reactions while nonspecific sorption involves coulombic forces generally depends on the aqueous pH and the pH_{PZC} of the adsorbent. The pH dependence on the phosphate removal of Z-Al (Figure 3) shows the lowest phosphate removal at pH below than 2; and the highest with a plateau between pH 3 and 6 to decreases then from pH 6 to 11.

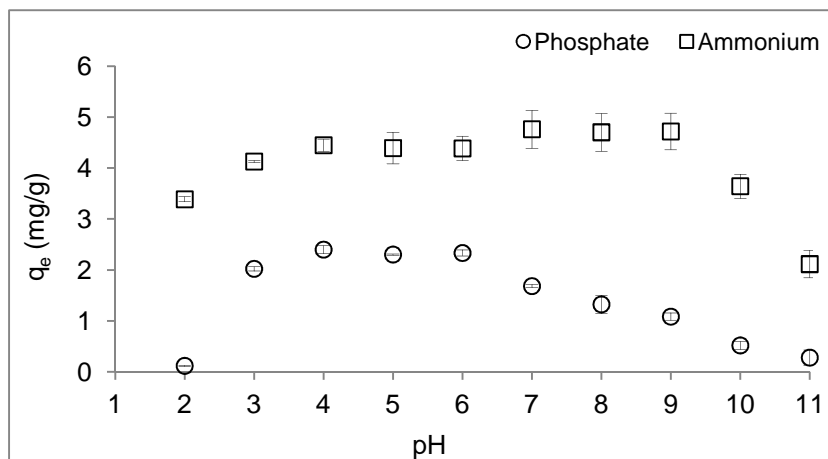
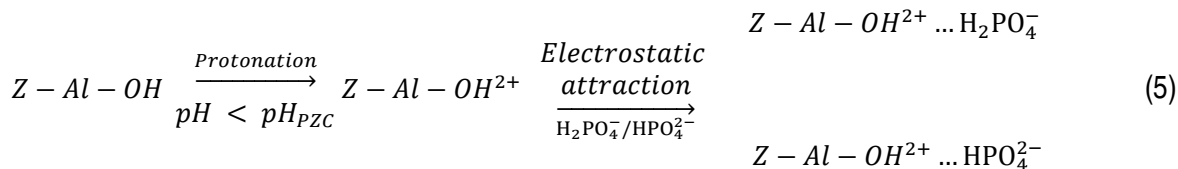
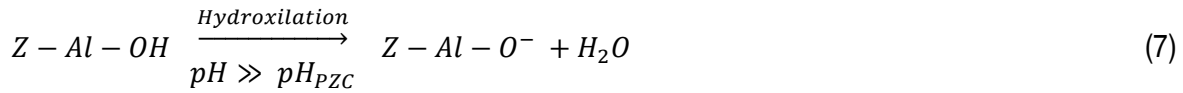
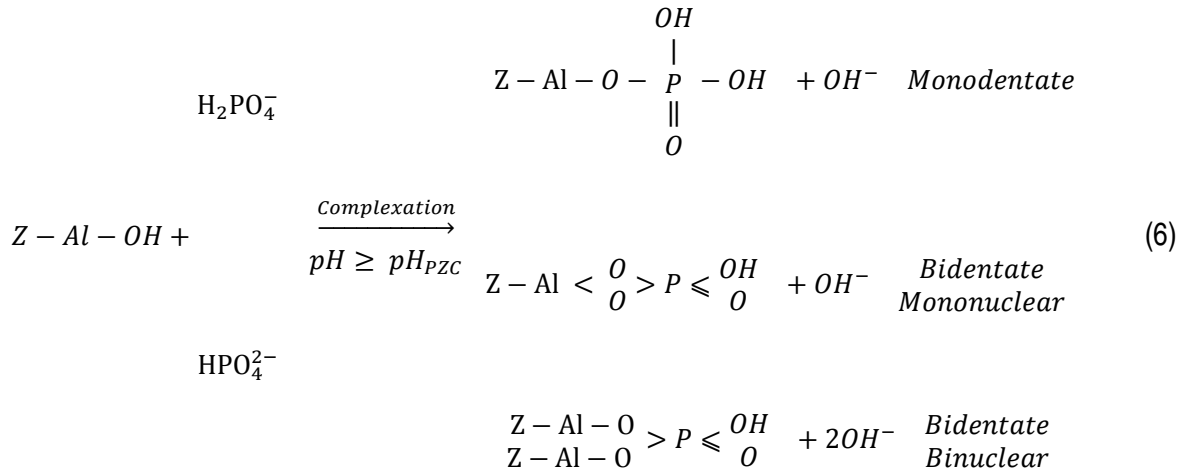


Figure 3. Effect of pH on the phosphate and ammonium removal by the hybrid hydrated aluminum oxide zeolite (Z-Al).

The sorption mechanism of phosphate oxyanions ($\text{H}_2\text{PO}_4^- - \text{HPO}_4^{2-} - \text{PO}_4^{3-}$) is associated with the formation of complexes with the hydroxyl surface groups of the hydrated aluminum oxide layer impregnated on the zeolite structure (specific adsorption) [17, 43-45] or by means of columbic forces depending of the pH_{PZC} (non-specific adsorption) [13, 23, 45].

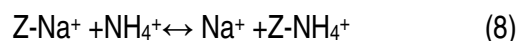
Then, taking into account that pH_{PZC} of the aluminum hydrated oxide in Z- Al was found to be 4.5 ± 0.2 , below the pH_{PZC} , the Z-Al surface is positively-charged, which becomes an opportunity for anions sorption as is depicted in Eq. 5. However, the reduction of pH below 2.3 ($\text{pK}_{\text{a}1}$) favours the conversion of H_2PO_4^- to H_3PO_4 and therefore the anion exchange mechanism is not favoured as phoshate is a non-charged form. Instead, above the pH_{PZC} the adsorbent surface is negatively-charged (Eq. 7) and anions sorption is not favourable.





At $\text{pH} \geq \text{pH}_{\text{PZC}}$ the Al-OH groups are involved in the formation of inner sphere species by means of monodentate and bidentate complexation (Eq. 6) [17, 46, 47]. Then, an increase of pH above 11 is traduced in the gradual conversion of the HPO_4^{2-} onto PO_4^{3-} and consequently, a reduction of the phosphate removal. The reduction is associated to both, the high charge of the ion (-3) and the fact that the hydrated hydroxide surface is negatively charged ($\cong\text{AlO}^-$).

The ammonium sorption by Z-Al (Figure 3) increases progressively from pH 2 until 9. Below the pH_{PZC} the existence of positive charges on the Z-Al surface is the responsible for a reduction of the ammonium removal. On other hand, above the pH_{PZC} the increase of ammonium (NH_4^+) sorption is attributed to the electrostatic interaction with the deprotonated surface groups ($\cong\text{AlO}^-$). The decrease of ammonium sorption at pH 10 is associated with the decrease of the NH_4^+ concentration as it is converted to the NH_3 . So, the ion exchange reaction on a sodium zeolite is described as a chemical process involving valence forces through the sharing or exchange of electrons between zeolite sites with negative charge and ammonium cations as described by Eq. 8 [5, 48]:



Analysis of the aqueous phase (data not reported) confirm the release of Na^+ and in minor degree of K^+ , Mg^{2+} , Ca^{2+} . SEM data revealed the reduction of these cations in the ammonium loaded Z-Al.

3.3. Effect of competing ions on ammonium and phosphate sorption

Sorption capacity of Z-Al for both phosphate and ammonium in the presence of common anions and cations in treated waste water is shown in Figure 4. The ammonium sorption capacity was maintained as the variations were below 5 %. A similar effect was confirmed for phosphate uptake in the presence of nitrate, sulfate and chloride as reported for other zeolitic materials [1, 48]. These species are mainly supposed to form outer-sphere complexes and they do not represent any competition for the same binding sites [2, 49]. The presence of HCO_3^- was found to promote the reduction of 32 % on the phosphate uptake as reported for a modified zeolite [50]. The combined effect of anions revealed the decrease of phosphate and ammonium removal of 29 % and 9 %, respectively.

The evaluation of the effect of cations towards ammonium uptake by Z-Al revealed an important decrease for K^+ (17 %) > Ca^{2+} (15 %) > Na^+ (12 %) > Mg^{2+} (6 %) as was previously reported with natural zeolites [48]. Contrary, no significant differences were measured in phosphate sorption with differences below 5 % (e.g. Mg^{2+} (6 %) > Na^+ (3 %) > K^+ (3 %) and Ca^{2+} (1 %)). The combined effect of cations leads the reduction of phosphate and ammonium uptake of 3 % and 33 %, respectively.

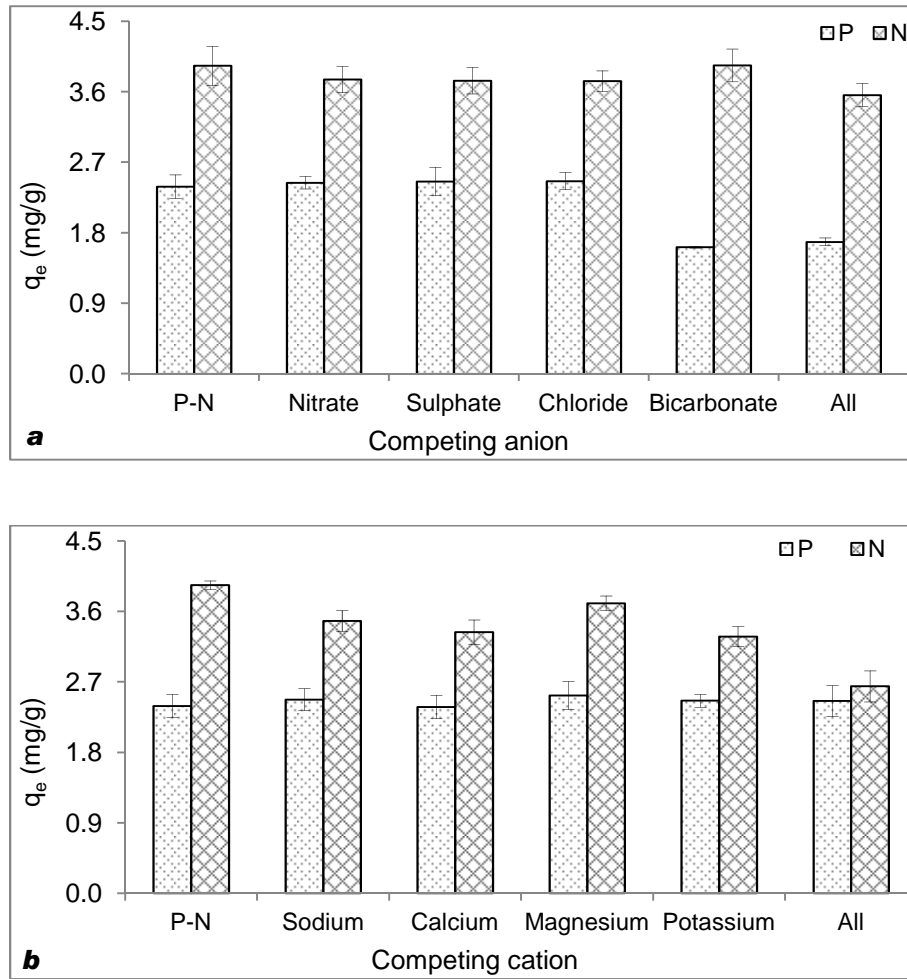


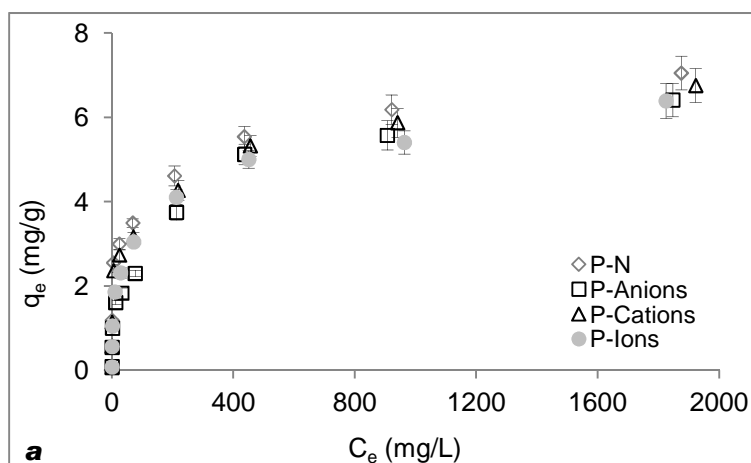
Figure 4. Individually effect of a) anions and b) cations for phosphate (P) and ammonium (N) removal onto the hybrid hydrated aluminum oxide zeolite (Z-Al).

The phosphate and ammonium equilibrium sorption by Z-Al in the presence of the anions and cations mixtures (Table 3) are better described by the Langmuir isotherm ($R^2 \geq 0.99$) than by the Freundlich isotherm ($R^2 \leq 0.84$). The maximum phosphate uptake capacity without competing ions (7.0 mg-P/g) was slightly reduced by the presence of ions mixtures to 6.3 mg-P/g, in the presence of anions to 6.4 mg-P/g and in the presence of cations to 6.7 mg-P/g. Similarly, the ammonium uptake capacity (30 mg-N/g) slightly decreased to 26 mg-N/g when all competing ions were present, to 27 mg-N/g in

presence of cations and to 28 mg-N/g in presence of anions. Phosphate and ammonium sorption data for Z-Al in the presence of competing ions at different concentrations are shown in Figure 5.

	Langmuir			Freundlich		
	q_m (mg/g)	K_L (L/mg)	R^2	K_F ((mg/g)/(mg/L) ^{1/n})	1/n	R^2
Phosphate (single)	7.0	0.02	0.99	0.85	0.32	0.85
P (Anions mixture)	6.4	0.01	0.98	0.52	0.36	0.93
P (Cations mixture)	6.7	0.02	0.99	0.78	0.32	0.84
P (Ions mixture)	6.3	0.02	0.99	0.59	0.36	0.86
Ammonium (single)	30	0.011	0.99	2.64	0.32	0.92
N (Anions mixture)	28	0.008	0.99	1.62	0.39	0.91
N (Cations mixture)	27	0.009	0.99	1.25	0.42	0.92
N (Ions mixture)	26	0.007	0.99	0.93	0.47	0.87

Table 3. Isotherm parameters for phosphate and ammonium sorption by hybrid hydrated aluminum oxide zeolite Z-Al in the presence of competing ions.



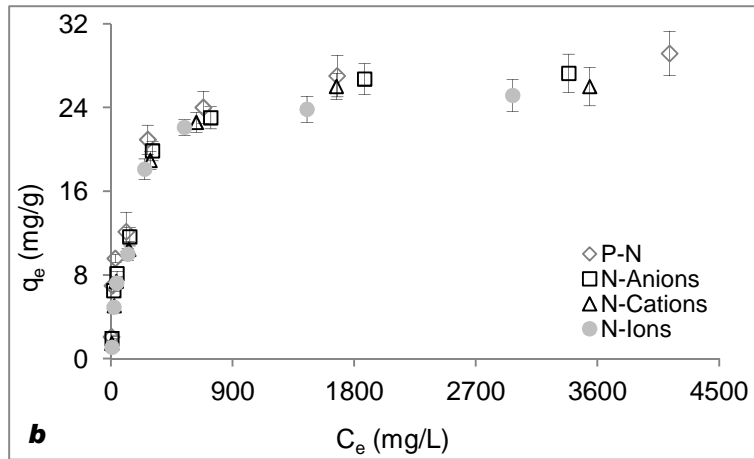


Figure 5. Equilibrium capacity for a) phosphate and b) ammonium in presence of competing ions with the hybrid hydrated aluminum oxide zeolite (Z-Al).

3.4. Phosphate and ammonium sorption kinetics

Kinetic data of both phosphate and ammonium removal by Z-Al are similar to those typically shown by polymeric ion exchangers as it is shown in Figure 6. More than 150 minutes were needed to reach the equilibrium, however; ammonium shows faster sorption rate than phosphate. This observation is attributable to the fact that the exchange of Na^+ by NH_4^+ ions is a faster process than the complexation of phosphate ions with the surfaces groups ($\cong\text{AlOH}$).

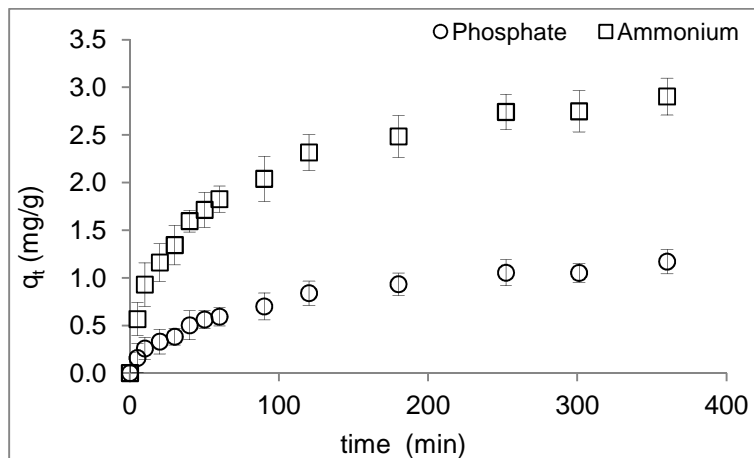


Figure 6. Evolution of phosphate and ammonium sorption uptake versus time for Z-Al in batch experiments at 21 ± 1 °C.

The kinetic data of phosphate and ammonium sorption onto modified zeolite were fitted to the pseudo-first order and pseudo-second order kinetic model by Eq. 9 and Eq. 10.

$$\ln(q_e - q_t) = \ln(q_e) - k_1 t \quad (9)$$

$$\frac{t}{q_t} = \frac{1}{k_2 q_e^2} + \frac{t}{q_e} \quad (10)$$

where k_1 (h^{-1}) and k_2 ($\text{g.mg}^{-1}.\text{h}^{-1}$) are the kinetics constants. The pseudo-second order model provided a good description for phosphate and ammonium sorption. However, the intraparticle diffusion model developed by Weber and Morris [51] also was used for describing sorption processes on the zeolite. The mathematical dependence of uptake q_t of adsorbates on $t^{1/2}$ is obtained if the sorption process is considered to be influenced by diffusion in the spherical adsorbent and by convective diffusion in the adsorbate solution. This dependence is described by the Eq. 11:

$$q_t = k_t t^{1/2} + A \quad (11)$$

where k_t ($\text{mg.g}^{-1}.\text{h}^{-1/2}$) is the intraparticle diffusion rate constant and A (mg/g) is a constant providing an indication of the thickness of the boundary layer, i.e. the higher the value of A , the greater the boundary layer effect. If the sorption uptake q_t is plotted versus $t^{1/2}$ gives a straight line, this means that the sorption process is only controlled by intraparticle diffusion. However, two or more steps influence the sorption process if the data exhibit multi-linear plots.

The intra-particle diffusion model fitted well the experimental data as can be seen in Figure 7 indicating that the whole sorption process is divided into two linear regions. Hence, the ammonium

and phosphate sorption process might be described by film diffusion followed by particle diffusion process [52].

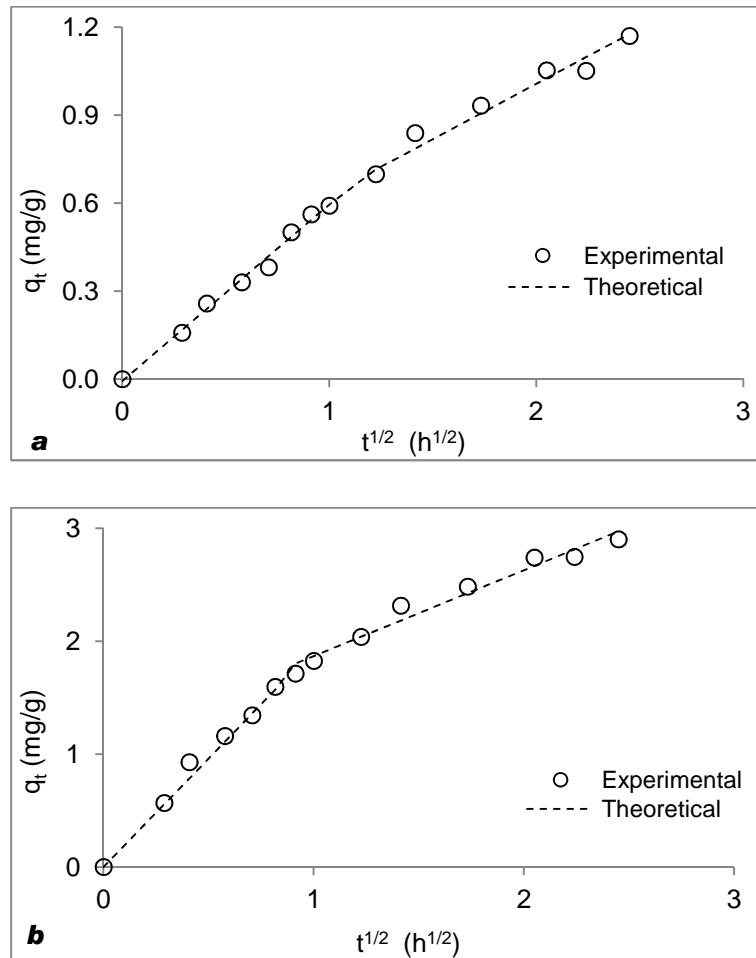


Figure 7. Intra-particle diffusion plots for a) phosphate and b) ammonium removal by hybrid hydrated aluminum oxide zeolite (Z-Al).

The contribution of each rate controlling step in the phosphate and ammonium sorption onto Z-Al can be further analyzed through the homogenous particle diffusion model (HPDM) and film diffusion model (HPDF) by calculating the film diffusion (D_f) and particle diffusion (D_p) [53]. In this model the species originally in the solution phase must diffuse across the liquid film surrounding the adsorbent particle, transfer across the solution/ particle interface, diffuse into the bulk of the adsorbent particle

and possibly interact with a moiety on the surface of the adsorbent [54]. Sorption on spherical particles under particle diffusion control is described by Eq. 12:

$$-\ln \left(1 - \left(\frac{q_t}{q_e} \right)^2 \right) = \frac{2 \pi^2 D_p}{r^2} t \quad (12)$$

If liquid film diffusion controls the rate of sorption is described by Eq. 13:

$$-\ln \left(1 - \left(\frac{q_t}{q_e} \right)^2 t \right) = \frac{D_f C_s}{h r C_z} t \quad (13)$$

where q_t and q_e are solute uptake on the adsorbent phase at time t and when equilibrium is attained (mg/g) respectively and C_s and C_z (mg/kg) are the concentrations of solute in solution and in the zeolite, respectively; r is the average radius of zeolite particles (1×10^{-4} m), t is the contact time (min or s); and h is the thickness of film around the zeolite particle (1×10^{-5} m for poorly stirred solution) [55].

Kinetic experimental data were fitted to equations 12 and 13 and D_p and D_f values for ammonia and phosphate sorption onto Z-Al as well as the linear regression analysis are summarized in Table 4. The D_p values for both ions were considerably lower than those of D_f , indicating that particle diffusion was the rate-limiting step for both ions and their sorption was mainly occurred at the surface of zeolite with monolayer molecular adsorption. Similar results were reported for natural zeolites [52, 55, 56] at low initial ammonium concentrations.

Model	Kinetic parameters	Phosphate	Ammonium
Pseudo-first order	q_e (mg·g ⁻¹)	1.4	2.6
	k_1 (h ⁻¹)	0.2	0.3
	R^2	0.93	0.91
Pseudo-second order	q_e (mg·g ⁻¹)	1.3	3.1
	k_2 (g·mg ⁻¹ ·h ⁻¹)	0.6	0.1
	R^2	0.99	1.00
Intraparticle diffusion	k_{t1} (mg·g ⁻¹ ·h ^{-1/2})	0.6	1.9
	R^2	0.99	0.99

	k_{t2} (mg·g ⁻¹ ·h ^{-1/2})	0.4	0.8
	R ²	0.97	0.97
HPDF	D_f (m ² ·s ⁻¹)	4.9x10 ⁻¹⁰	9.9x10 ⁻¹⁰
Film diffusion	R ²	0.93	0.91
HPDM	D_f (m ² ·s ⁻¹)	8.8x10 ⁻¹³	1.5x10 ⁻¹²
Particle diffusion	R ²	0.98	0.97

Table 4. Kinetic parameters for phosphate and ammonium removal by hybrid hydrated aluminum oxide zeolite (Z-Al).

FSEM analyses of loaded phosphate and ammonium Z-Al revealed that the surface is almost covered by several lamellar particles (supporting information Figure S2d) and EDAX analysis of the loaded adsorbent revealed the presence of phosphorous. Nitrogen was not detected as the content is below the limit of quantification. The size of the cavities in the unload material decreased with the sorption process. Then the surface turned to be a compact crystalline framework. The FTIR analysis performed after the phosphate and ammonium sorption (Figure 8) showed changes in bands at 3616 cm⁻¹, 1015 cm⁻¹ and the appearance of a new band at 1436 cm⁻¹. These variations are associated with the participation of hydroxyl groups of Al(OH) by means complexation with phosphate and ammonium when sorption has taken place over zeolite surface [57-60]. This fact may explain the phosphate and ammonium ions competition for the same binding sites. It explains the increase of the phosphate removal leading the slight reduction of the ammonium sorption capacity as it occurred in natural as well as modified zeolite.

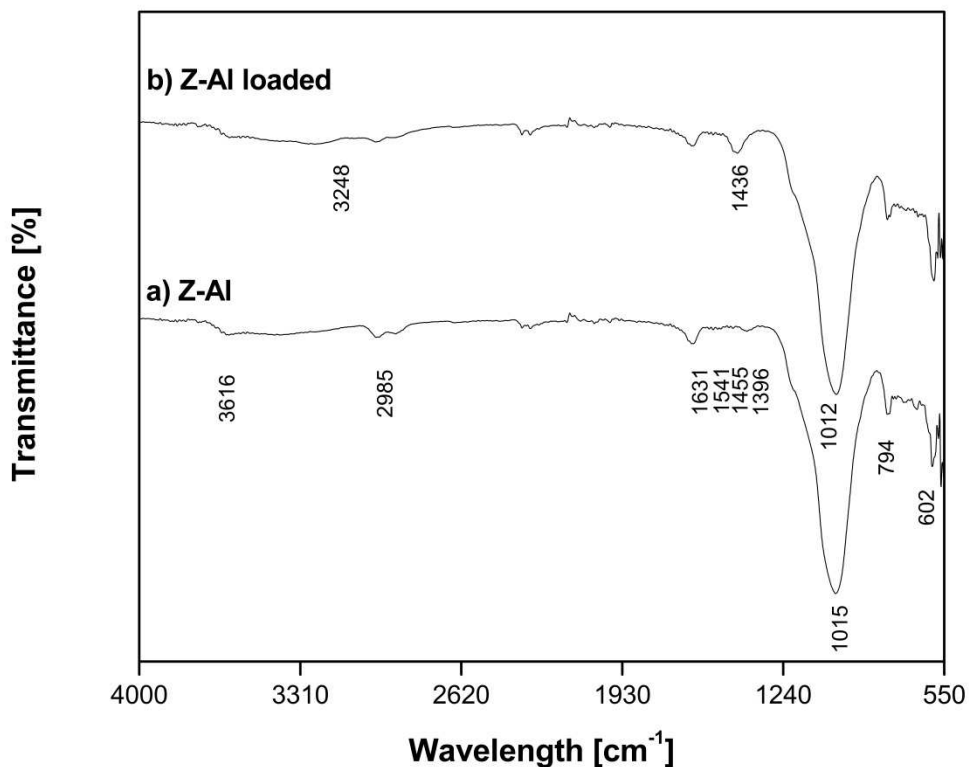


Figure 8. FTIR of the zeolitic materials a) unloaded hybrid hydrated aluminum oxide zeolite (Z-Al) and b) P and N loaded Z-Al.

3.5. Phosphate speciation in loaded Z-Al samples

Phosphate speciation results are collected in Table 5. For Z-Al the content of residual phosphorus (R-P) was found to be 9 ± 3 %. The loosely bound phosphorus fraction (LB-P) was found to be 4 ± 1 % as reported for a synthetic zeolite [6]. The major phosphorus fraction retained by Z-Al was associated to Al and Fe hydroxides (Fe+Al)-P which represent the 53 ± 1 %. Thus, it revealed the Al-OH groups of the hydrated aluminum oxides in the modified zeolite Z-Al to be the main responsible for the phosphate removal. Finally, the 35 ± 3 % of phosphorus immobilized was related to calcium and magnesium (Ca+Mg)-P fraction. Then, phosphate removal is also performed by means of chemical

precipitation with these cationic species; although these mineral phases were not identified by XRD analysis.

q_e (mg/g)	LB-P		(Fe+Al)-P		(Ca+Mg)-P		R-P	
	(mg/g)	%	(mg/g)	%	(mg/g)	%	(mg/g)	%
2.04	0.1	4±1	1.0	53±1	0.7	35±3	0.2	9±3

Table 5. Fractionation of phosphate immobilized on the hybrid hydrated aluminum oxide zeolite (Z-Al) associated to the different chemical forms: LB-P; (Fe+Al)-P; (Ca+Mg)-P; R-P.

3.6. Phosphate and ammonium desorption

Desorption efficiency of phosphate and ammonium from loaded zeolites using NaOH, NaHCO₃, Na₂CO₃, and mixtures of NaHCO₃/Na₂CO₃ in the first sorption – desorption cycle are summarized in

Table 6:

Elution solution	Desorption (%)	
	Phosphate	Ammonium
1 M NaOH	20±3	83±4
0.1 M NaHCO ₃	24±3	50±4
0.1 M Na ₂ CO ₃	79±3	92±4
0.1 M NaHCO ₃ /0.1 M Na ₂ CO ₃	64±3	76±4

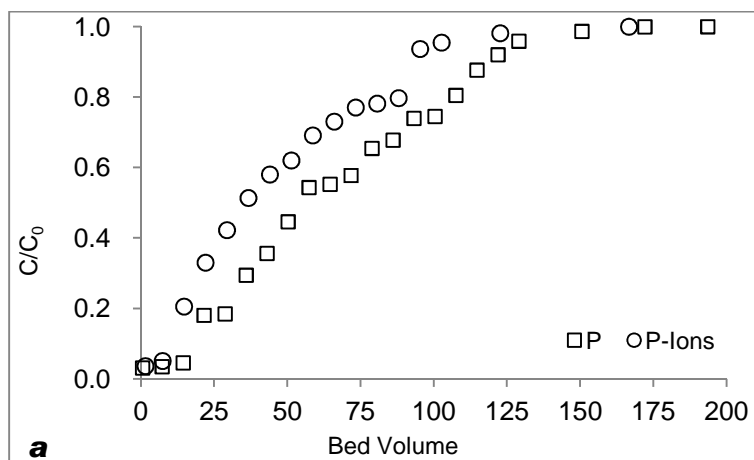
Table 6. Desorption efficiency of phosphate and ammonium from loaded Z-Al in batch experiments at 21±°C.

Ammonium is much better desorbed than phosphate with high recoveries from 50 up to 92 % for most of the elution solutions used while phosphate recovery varied from 20 up to 79 % in the first sorption – desorption cycle. The strong phosphate complexation with the hydrated aluminum oxide seems to be the responsible for this irreversible sorption. However, in the second sorption cycle it was found a strong reduction of phosphate capacity (≈96 %) in contrast to the slight variation in

ammonium removal of all four regenerated Z-Al samples. Concentrated alkaline solutions promote the dissolution of the hydrated oxide aluminum [61] as well as the partial dissolution of the zeolite structure as it has been postulated [38]. Although, the regeneration using NaOH solutions have been proposed effective for oxyanions from zeolites [61] scarce data could be found in literature as typically these materials were not developed for regeneration purposes. According to these results, and taking into account that ammonium and phosphate are not efficiently desorbed it is necessary to evaluate the possibility of direct used of the loaded zeolites for soils quality improvement.

3.7. Simultaneous removal of ammonium and phosphate in column tests

The breakthrough curves of the simultaneous phosphate and ammonium sorption by Z-Al in absence and presence of competing ions are shown in Figure 9. The breakthrough point ($C/C_0 = 0.05$) for phosphate and ammonium sorption was found at 15 BV instead in the presence of competing ions was 7 BV. The phosphate maximum sorption capacity reached at column saturation ($C/C_0 = 0.95$) was 5 mg-P/g at 194 BV, contrary in the presence of competing ions it decreased to 3 mg-P/g at 137 BV. Similarly behavior was found for ammonium sorption capacity with 28 mg-N/g at 430 BV in absence of competing ions and 16 mg-N/g at 211 BV in presence of interferences.



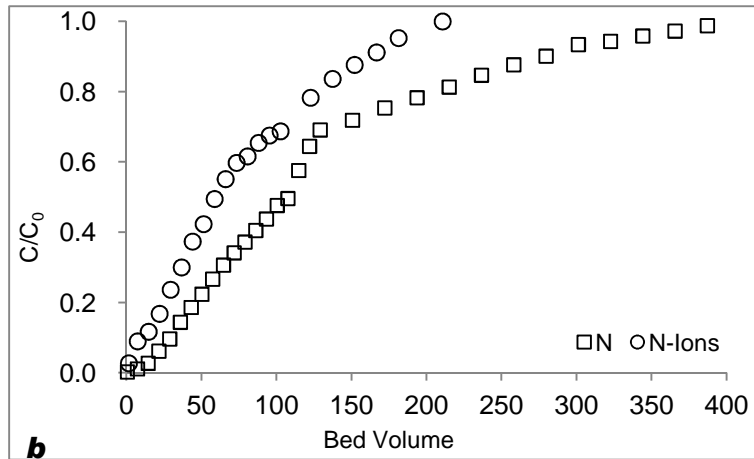
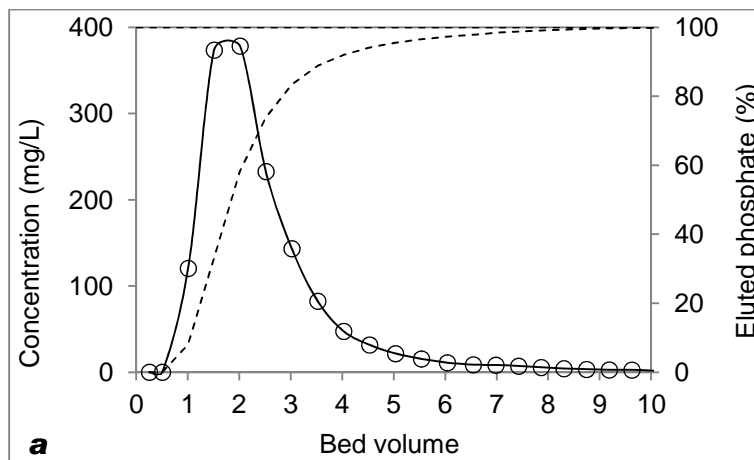


Figure 9. Breakthrough curves of a) phosphate and b) ammonium sorption by the hybrid hydrated aluminum oxide zeolite (Z-Al) with and without competing ions at EBHRT of 4 minutes.

The simultaneous phosphate and ammonium desorption from Z-Al was performed using 1 M NaOH solution after column operation in absence of competing ions. The profiles of ammonium and phosphate desorption are shown in Figure 10. The highest phosphate concentration was found to be 378 mg-P/L. Almost, the 90 % of the eluted phosphate was recovered within 4 BV. On the other hand the highest ammonium concentration was 3538 mg-N/L. The 95 % of the eluted ammonium was found at 3.5 BV. Under, these conditions enrichment factors of 50 and 120 for phosphate and ammonium respectively were achieved.



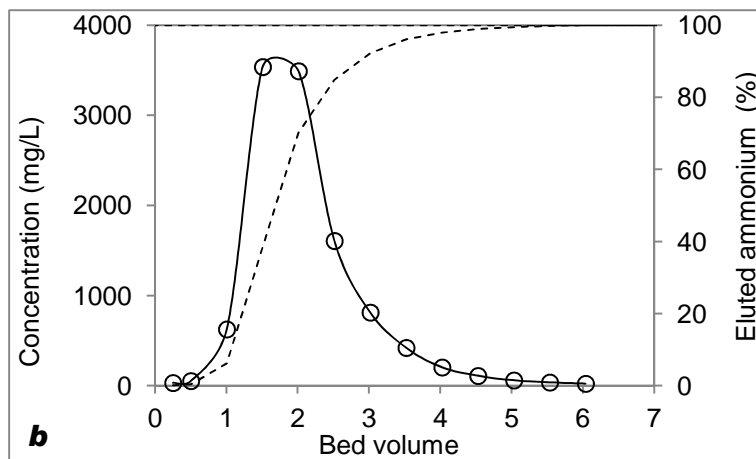


Figure 10. Column desorption profiles of a) phosphate and b) ammonium onto the hybrid hydrated aluminum oxide zeolite (Z-Al) using 1 M NaOH at EBHRT of 13 minutes.

4. Conclusions

The modification of a natural zeolite to produce a hybrid material containing hydrated aluminum oxide for phosphate recovery is not affecting its ammonium exchange capacity. Removal of phosphate is based on electrostatic interaction and the formation of inner sphere complexes with $\equiv\text{Al-OH}$ groups, while ammonium removal occurs by means of ion exchange and complexation with the OH groups of the zeolite. Both phosphate and ammonium sorption by Z-Al were well described by the Langmuir isotherm. Sorption capacity of both ions was slightly reduced when competing ions were present. Regeneration of the loaded zeolite using alkaline solutions containing sodium (NaOH, NaHCO_3 and Na_2CO_3) provided higher recoveries ratios for ammonium than for phosphate. Concentration factors about 50 and 120 for phosphate and ammonium, respectively using NaOH as elution solution were achieved. A reduction of phosphate sorption capacity was observed in reuse (sorption-desorption cycle) experiments, indicating that their applications for sorption – desorption operation can be limited and suggesting the direct valorization of the loaded zeolites as soil amendment.

Acknowledgments

This research was financially supported by Ministry of Science and Innovation through the ZERODISCHARGE project (CPQ2011-26799) and the Catalan government (project ref. 2009SGR905, 2014SGR050). The authors gratefully acknowledge R. Estany (Aigues de Barcelona), M. Gullom (EMMA), I. Sancho (Centro Tecnológico del Agua (CETaqua)), Zeocem (Slovakia) for zeolites supply. Finally, I. Lopez (Laboratory of Electronic Microscopy, Universitat Politècnica de Catalunya) for the FSEM analysis and to N. Moreno (IDAEA-CSIC) for XRD determinations. Diana Guaya acknowledges the financial support Secretaría de Educación Superior, Ciencia, Tecnología e Innovación (Senescyt - Ecuador) and Universidad Técnica Particular de Loja - Ecuador (Project - 2014: PROY_QUI_826).

References

- [1] M. Zhang, H. Zhang, D. Xu, L. Han, D. Niu, B. Tian, J. Zhang, L. Zhang, W. Wu, Removal of ammonium from aqueous solutions using zeolite synthesized from fly ash by a fusion method, *Desalination* 271 (2011) 111-121.
- [2] Q. Guan, X. Hu, D. Wu, X. Shang, C. Ye, H. Kong, Phosphate removal in marine electrolytes by zeolite synthesized from coal fly ash, *Fuel* 88 (2009) 1643-1649.
- [3] N. Widiastuti, H. Wu, H.M. Ang, D. Zhang, Removal of ammonium from greywater using natural zeolite, *Desalination* 277 (2011) 15-23.
- [4] R. Malekian, J. Abedi-Koupai, S.S. Eslamian, S.F. Mousavi, K.C. Abbaspour, M. Afyuni, Ion-exchange process for ammonium removal and release using natural Iranian zeolite, *Appl. Clay Sci.* 51 (2011) 323-329.
- [5] X. Chen, K. Wendell, J. Zhu, J. Li, X. Yu, Z. Zhang, Synthesis of nano-zeolite from coal fly ash and its potential for nutrient sequestration from anaerobically digested swine wastewater, *Bioresour. Technol.* 110 (2012) 79-85.

- [6] J. Xie, Z. Wang, D. Wu, Z. Zhang, H. Kong, Synthesis of Zeolite/Aluminum Oxide Hydrate from Coal Fly Ash: A New Type of Adsorbent for Simultaneous Removal of Cationic and Anionic Pollutants, *Ind. Eng. Chem. Res.* 52 (2013) 14890-14897.
- [7] J. Xie, Z. Wang, D. Wu, H. Kong, Synthesis and properties of zeolite/hydrated iron oxide composite from coal fly ash as efficient adsorbent to simultaneously retain cationic and anionic pollutants from water, *Fuel* 116 (2014) 71-76.
- [8] K.S. Kim, J.O. Park, S.C. Nam, Synthesis of Iron-loaded Zeolites for Removal of Ammonium and Phosphate from Aqueous Solutions, *Environ Eng Res* 18 (2013) 267-276.
- [9] Q. Du, S. Liu, Z. Cao, Y. Wang, Ammonia removal from aqueous solution using natural Chinese clinoptilolite, *Sep. Purif. Technol.* 44 (2005) 229-234.
- [10] R. Leyva-Ramos, G. Aguilar-Armenta, L.V. Gonzalez-Gutierrez, R.M. Guerrero-Coronado, J. Mendoza-Barron, Ammonia exchange on clinoptilolite from mineral deposits located in Mexico, *J. Chem. Technol. Biotechnol.* 79 (2004) 651-657.
- [11] M. Król, W. Mozgawa, W. Jastrzębski, K. Barczyk, Application of IR spectra in the studies of zeolites from D4R and D6R structural groups, *Microporous Mesoporous Mater.* 156 (2012) 181-188.
- [12] C. Jiang, L. Jia, Y. He, B. Zhang, G. Kirumba, J. Xie, Adsorptive removal of phosphorus from aqueous solution using sponge iron and zeolite, *J. Colloid Interface Sci.* 402 (2013) 246-252.
- [13] E.B. Simsek, E. Özdemir, U. Beker, Zeolite supported mono- and bimetallic oxides: Promising adsorbents for removal of As(V) in aqueous solutions, *Chem. Eng. J.* 220 (2013) 402-411.
- [14] M.J. Jiménez-Cedillo, M.T. Olguín, C. Fall, Adsorption kinetic of arsenates as water pollutant on iron, manganese and iron–manganese-modified clinoptilolite-rich tuffs, *J. Hazard. Mater.* 163 (2009) 939-945.

- [15] M.J. Jiménez-Cedillo, M.T. Olgúin, C. Fall, A. Colín, Adsorption capacity of iron- or iron–manganese-modified zeolite-rich tuffs for As(III) and As(V) water pollutants, *Appl. Clay Sci.* 54 (2011) 206-216.
- [16] A. Alshameri, C. Yan, X. Lei, Enhancement of phosphate removal from water by TiO₂/Yemeni natural zeolite: Preparation, characterization and thermodynamic, *Microporous Mesoporous Mater.* 196 (2014) 145-157.
- [17] J. Lů, H. Liu, R. Liu, X. Zhao, L. Sun, J. Qu, Adsorptive removal of phosphate by a nanostructured Fe–Al–Mn trimetal oxide adsorbent, *Powder Technol.* 233 (2013) 146-154.
- [18] L. Gómez-Hortigüela, J. Pérez-Pariente, R. García, Y. Chebude, I. Díaz, Natural zeolites from Ethiopia for elimination of fluoride from drinking water, *Sep. Purif. Technol.* 120 (2013) 224-229.
- [19] P. Vassileva, D. Voikova, Investigation on natural and pretreated Bulgarian clinoptilolite for ammonium ions removal from aqueous solutions, *J. Hazard. Mater.* 170 (2009) 948-953.
- [20] R.M.A. Tehrani, A.A. Salari, The study of dehumidifying of carbon monoxide and ammonia adsorption by Iranian natural clinoptilolite zeolite, *Appl. Surf. Sci.* 252 (2005) 866-870.
- [21] M.E. Villanueva, A. Salinas, G.J. Copello, L.E. Díaz, Point of zero charge as a factor to control biofilm formation of *Pseudomonas aeruginosa* in sol-gel derivatized aluminum alloy plates, *Surf. Coat. Technol.* 254 (2014) 145-150.
- [22] J. Sarma, S. Mahiuddin, Specific ion effect on the point of zero charge of α -alumina and on the adsorption of 3,4-dihydroxybenzoic acid onto α -alumina surface, *Colloids Surf., A* 457 (2014) 419-424.
- [23] H.R. Zebardast, M. Pawlik, S. Rogak, E. Asselin, Potentiometric titration of hematite and magnetite at elevated temperatures using a ZrO₂-based pH probe, *Colloids Surf., A* 444 (2014) 144-152.

- [24] Y. Liu, R. Naidu, H. Ming, Surface electrochemical properties of red mud (bauxite residue): Zeta potential and surface charge density, *J. Colloid Interface Sci.* 394 (2013) 451-457.
- [25] K. Khawmee, A. Suddhiprakarn, I. Kheoruenromne, B. Singh, Surface charge properties of kaolinite from Thai soils, *Geoderma* 192 (2013) 120-131.
- [26] R.E. Martinez, O.S. Pokrovsky, J. Schott, E.H. Oelkers, Surface charge and zeta-potential of metabolically active and dead cyanobacteria, *J. Colloid Interface Sci.* 323 (2008) 317-325.
- [27] A.H.M. Hieltjes, L. Lijklema, Fractionation of Inorganic Phosphates in Calcareous Sediments¹, *J. Environ. Qual.* 9 (1980) 405-407.
- [28] A. APHA, WEF., Standard methods for the examination of water and wastewater, American Public Health Association, American Water Works Association, and Water Environment Federation, 2000.
- [29] L. Lei, X. Li, X. Zhang, Ammonium removal from aqueous solutions using microwave-treated natural Chinese zeolite, *Sep. Purif. Technol.* 58 (2008) 359-366.
- [30] M.K. Doula, Synthesis of a clinoptilolite–Fe system with high Cu sorption capacity, *Chemosphere* 67 (2007) 731-740.
- [31] H. Valdés, S. Alejandro, C.A. Zaror, Natural zeolite reactivity towards ozone: The role of compensating cations, *J. Hazard. Mater.* 227–228 (2012) 34-40.
- [32] K. Margeta, N.Z. Logar, M. Šiljeg, A. Farkaš, Natural Zeolites in Water Treatment – How Effective is Their Use, in: W. Elshorbagy, R.K. Chowdhury (Eds.) *Water Treatment*, InTech, Rijeka, 2013, pp. 81-112.
- [33] W. Stumm, *Chemistry of the solid water interface: Processes at the mineral-water and water-particle interface in natural systems*, Wiley and Sons Inc. 1992.

- [34] M. Reháková, L. Fortunová, Z. Bastl, S. Nagyová, S. Dolinská, V. Jorík, E. Jóna, Removal of pyridine from liquid and gas phase by copper forms of natural and synthetic zeolites, *J. Hazard. Mater.* 186 (2011) 699-706.
- [35] J. Li, J. Qiu, Y. Sun, Y. Long, Studies on natural STI zeolite: modification, structure, adsorption and catalysis, *Microporous Mesoporous Mater.* 37 (2000) 365-378.
- [36] F. Jin, Y. Li, A FTIR and TPD examination of the distributive properties of acid sites on ZSM-5 zeolite with pyridine as a probe molecule, *Catal. Today* 145 (2009) 101-107.
- [37] S. Alejandro, H. Valdés, M.-H. Manéro, C.A. Zaror, Oxidative regeneration of toluene-saturated natural zeolite by gaseous ozone: The influence of zeolite chemical surface characteristics, *J. Hazard. Mater.* 274 (2014) 212-220.
- [38] A. Alshameri, A. Ibrahim, A.M. Assabri, X. Lei, H. Wang, C. Yan, The investigation into the ammonium removal performance of Yemeni natural zeolite: Modification, ion exchange mechanism, and thermodynamics, *Powder Technol.* 258 (2014) 20-31.
- [39] Z. Luan, J.A. Fournier, In situ FTIR spectroscopic investigation of active sites and adsorbate interactions in mesoporous aluminosilicate SBA-15 molecular sieves, *Microporous Mesoporous Mater.* 79 (2005) 235-240.
- [40] X.-w. Cheng, Y. Zhong, J. Wang, J. Guo, Q. Huang, Y.-c. Long, Studies on modification and structural ultra-stabilization of natural STI zeolite, *Microporous Mesoporous Mater.* 83 (2005) 233-243.
- [41] E. Brunner, Solid state NMR — a powerful tool for the investigation of surface hydroxyl groups in zeolites and their interactions with adsorbed probe molecules, *J. Mol. Struct.* 355 (1995) 61-85.
- [42] K.Y. Foo, B.H. Hameed, Insights into the modeling of adsorption isotherm systems, *Chem. Eng. J.* 156 (2010) 2-10.

- [43] D. Dzombak, F. Morel, *Surface Complexation Modeling: Hydrous Ferric Oxide*, John Wiley & Sons, Inc., New York, 1990.
- [44] L.M. Blaney, S. Cinar, A.K. SenGupta, Hybrid anion exchanger for trace phosphate removal from water and wastewater, *Water Res.* 41 (2007) 1603-1613.
- [45] M.G. Sujana, G. Soma, N. Vasumathi, S. Anand, Studies on fluoride adsorption capacities of amorphous Fe/Al mixed hydroxides from aqueous solutions, *J. Fluorine Chem.* 130 (2009) 749-754.
- [46] Y. Su, H. Cui, Q. Li, S. Gao, J.K. Shang, Strong adsorption of phosphate by amorphous zirconium oxide nanoparticles, *Water Res.* 47 (2013) 5018-5026.
- [47] L.-g. Yan, Y.-y. Xu, H.-q. Yu, X.-d. Xin, Q. Wei, B. Du, Adsorption of phosphate from aqueous solution by hydroxy-aluminum, hydroxy-iron and hydroxy-iron–aluminum pillared bentonites, *J. Hazard. Mater.* 179 (2010) 244-250.
- [48] H. Huang, X. Xiao, B. Yan, L. Yang, Ammonium removal from aqueous solutions by using natural Chinese (Chende) zeolite as adsorbent, *J. Hazard. Mater.* 175 (2010) 247-252.
- [49] M.S. Onyango, D. Kuchar, M. Kubota, H. Matsuda, Adsorptive Removal of Phosphate Ions from Aqueous Solution Using Synthetic Zeolite, *Ind. Eng. Chem. Res.* 46 (2007) 894-900.
- [50] P. Ning, H.-J. Bart, B. Li, X. Lu, Y. Zhang, Phosphate removal from wastewater by model-La(III) zeolite adsorbents, *J. Environ. Sci.* 20 (2008) 670-674.
- [51] W.J. Weber, J.C. Morris, Kinetics of adsorption on carbon solution, *J. San. Eng. Div.* 89 (1963) 31-59.
- [52] L. Lin, Z. Lei, L. Wang, X. Liu, Y. Zhang, C. Wan, D.-J. Lee, J.H. Tay, Adsorption mechanisms of high-levels of ammonium onto natural and NaCl-modified zeolites, *Sep. Purif. Technol.* 103 (2013) 15-20.
- [53] F.G. Helfferich, *Ion exchange*, McGraw-Hill, New York, 1962.

- [54] C. Valderrama, J.I. Barios, M. Caetano, A. Farran, J.L. Cortina, Kinetic evaluation of phenol/aniline mixtures adsorption from aqueous solutions onto activated carbon and hypercrosslinked polymeric resin (MN200), *React. Funct. Polym.* 70 (2010) 142-150.
- [55] G. Moussavi, S. Talebi, M. Farrokhi, R.M. Sabouti, The investigation of mechanism, kinetic and isotherm of ammonia and humic acid co-adsorption onto natural zeolite, *Chem. Eng. J.* 171 (2011) 1159-1169.
- [56] M. Sprynskyy, M. Lebedynets, R. Zbytniewski, J. Namieśnik, B. Buszewski, Ammonium removal from aqueous solution by natural zeolite, Transcarpathian mordenite, kinetics, equilibrium and column tests, *Sep. Purif. Technol.* 46 (2005) 155-160.
- [57] H. Huang, D. Xiao, R. Pang, C. Han, L. Ding, Simultaneous removal of nutrients from simulated swine wastewater by adsorption of modified zeolite combined with struvite crystallization, *Chem. Eng. J.* 256 (2014) 431-438.
- [58] J. Guo, C. Yang, G. Zeng, Treatment of swine wastewater using chemically modified zeolite and bioflocculant from activated sludge, *Bioresour. Technol.* 143 (2013) 289-297.
- [59] M.A. Wahab, S. Jellali, N. Jedidi, Ammonium biosorption onto sawdust: FTIR analysis, kinetics and adsorption isotherms modeling, *Bioresour. Technol.* 101 (2010) 5070-5075.
- [60] M.A. Wahab, H. Boubakri, S. Jellali, N. Jedidi, Characterization of ammonium retention processes onto Cactus leaves fibers using FTIR, EDX and SEM analysis, *J. Hazard. Mater.* 241–242 (2012) 101-109.
- [61] Y.-H. Xu, T. Nakajima, A. Ohki, Adsorption and removal of arsenic(V) from drinking water by aluminum-loaded Shirasu-zeolite, *J. Hazard. Mater.* B92 (2002) 275-287.